Simulation of 2D ambient acoustics using linearized Euler Equations

Tanmay C. Shidhore and Tanmay C. Inamdar

West Lafayette, United States

1. Motivation

The objective of this project is to simulate acoustic propagation of a source placed in a 2D circular domain. A Gaussian pressure bump (radius of spread=0.1) with a sinusoidal time variation is considered as the disturbance/source and its time evolution is recorded on a circle of radius 3. A sponge boundary condition (with quadratic damping) is used to emulate a microphone, meant to capture the incoming acoustic waves.

2. Problem Geometry and Mesh

As mentioned previously,the geometry considered was a circle with radius 3 (see figure 1).

The total no. of control volumes in the mesh was 9170 and the mesh was entirely made up of triangular control volumes.

A pressure disturbance, given by equation is initialized

$$p(\vec{r},t) = 10^{-4}\rho_0 {a_0}^2 e^{\frac{-1}{(1-(r/r_0)^2)}} sin(2\pi f t) \tag{1}$$

where $r = |\vec{r}|$ is the radial distance from the centre of the circle and r_0 is the radial extent of the Gaussian bump, which is 0.1 in our case. Here, a_0 is the speed of sound and ρ_0 the density of the fluid (assumed to be unity for simplicity)

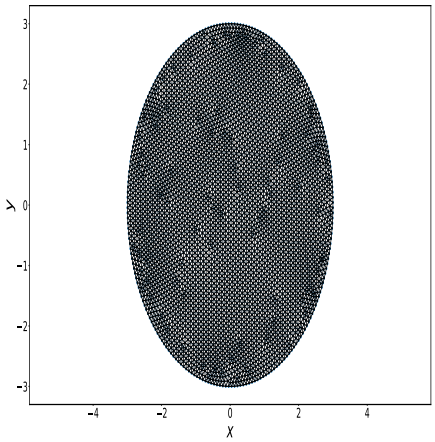

Figure 1: Mesh

3. Governing Equation

The physics of the problem is governed by the 2D linearized Euler equations-

$$\begin{aligned} \frac{dp}{dt} &= -\rho_0 {a_0}^2 \frac{\partial u_j}{\partial x_j} \\ \frac{du_j}{dt} &= -\frac{1}{\rho_0}\frac{p}{\partial x_j} \end{aligned} \tag{2}$$

Here, u_j is the j^{th} component of the velocity, p, the pressure and ρ_0, the density and a_0 the speed of sound and f the frequency of the pulse (also assumed to be unity for simplicity).

4. Boundary Conditions

The problem involved using a sponge boundary condition, which puts an additional source term on the RHS of equations (2) Thus, the new governing equations are:

$$\begin{aligned} \frac{dp}{dt} &= -\rho_0 {a_0}^2 \frac{\partial u_j}{\partial x_j} - K(r)[p - p_0] \\ \frac{du_j}{dt} &= -\frac{1}{\rho_0}\frac{p}{\partial x_j} - K(r)[u_j - u_{0j}] \end{aligned} \tag{3}$$

Here, u_{0j} and p_0 are the values of u_j and p expected to leave the domain (0 in the present case) and $K(r)$ is a damping function (the same for both equations for reasons of stability), resulting in the decay of p and u_j.

The damping function $K(r)$ can be modelled in several ways. This choice of function used to model the damping co-efficient heavily influences the radial thickness r_{sp} of the sponge. A constant K requires $r_{sp} \approx 15\lambda$ where λ is the wavelength of the disturbance. In order to use a more reasonable r_{sp} value ($\sim 0.3\lambda$), a quadratic damping function is used:

$$K(r) = (\frac{(r - 2.7)}{0.3})^2 \tag{4}$$

As seen from equation (4), the sponge layer starts at $r = 2.7$, with an initial value of 0, that quadratically increases to 1 at $r = 3$

5. Numerical Scheme and simulation parameters

The pressure was stored at the centre of the CVs and the velocity was computed at the cell faces. The spatial gradients were calculated using a least-squared fitting approach to obtain the corresponding derivative operators. The divergence was computed based on the Gauss theorem for each CV. Time advancement was done explicitly using a 4^{th} order Runge-Kutta method. The code also allows for a 2^{nd} and 1^{st} order Runge-Kutta method (by switching the corresponding flags in the code to 'True'). For this particular situation,

6. Results

Figures 2 through 13 show the pressure contours and velocity quiver plots at t=1,2,3,4,5 and 6 respectively

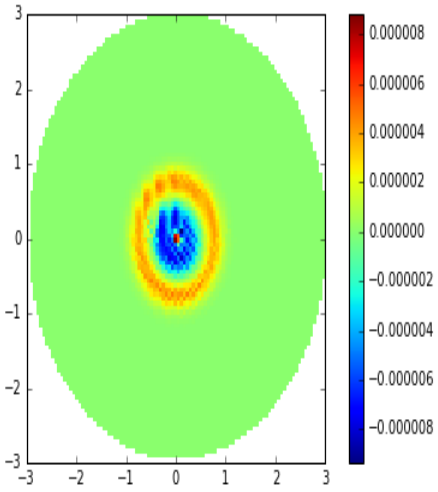

Figure 2: Pressure:t=1

A video (showing the time evolution) for $r_{sp} = 2.5$ and $r_0 = 0.5$has also been included in the report folder.

Furthermore, the pressure, at radial locations of 1, 1.5 and 2 was sampled (one point on the circle of radius 1,1.5 and 2 each) and plotted against the pressure at the centre of the source (scaled down by a factor of 10) (see figure 14

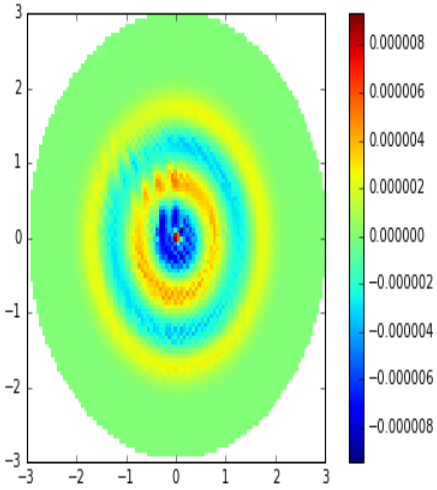

Figure 3: Pressure:t=2

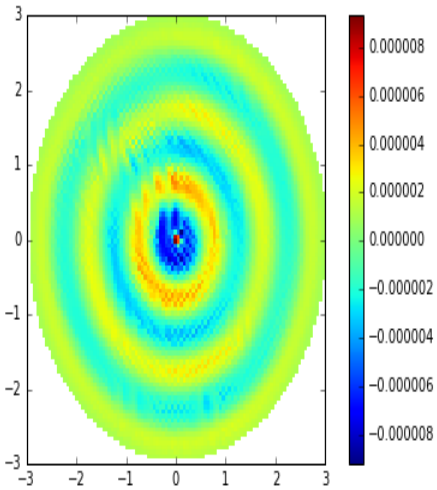

Figure 4: Pressure:t=3

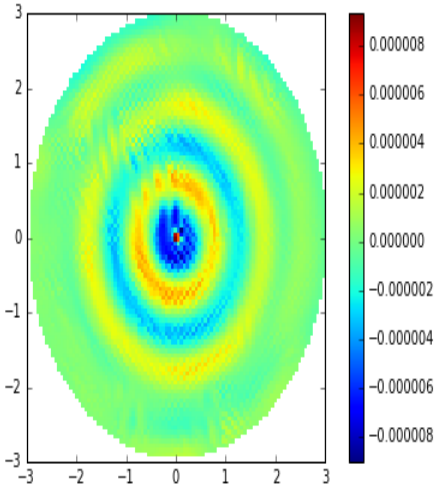

Figure 5: Pressure:t=4

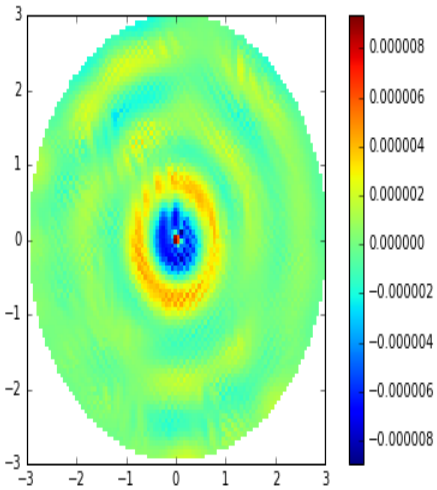

Figure 6: Pressure:t=5

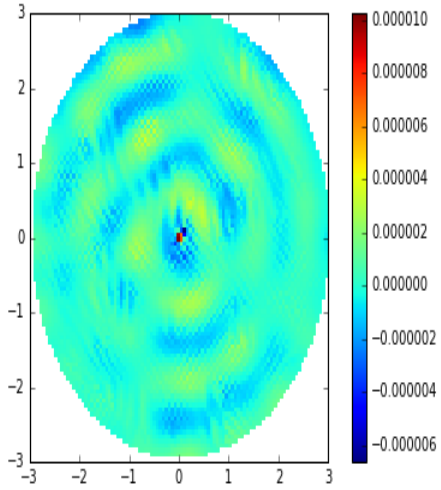

Figure 7: Pressure:t=6

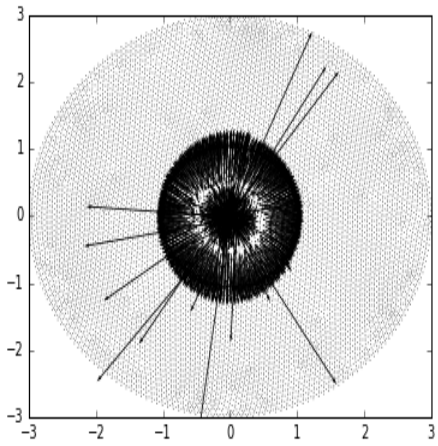

Figure 8: Velocity:t=1

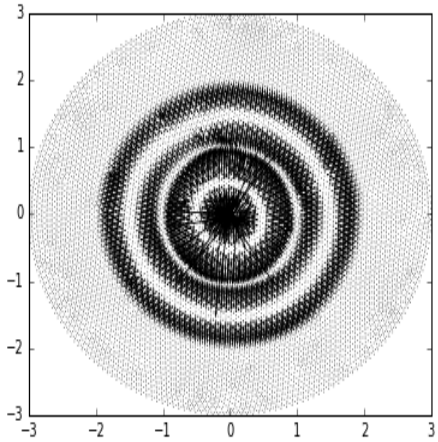

Figure 9: Velocity:t=2

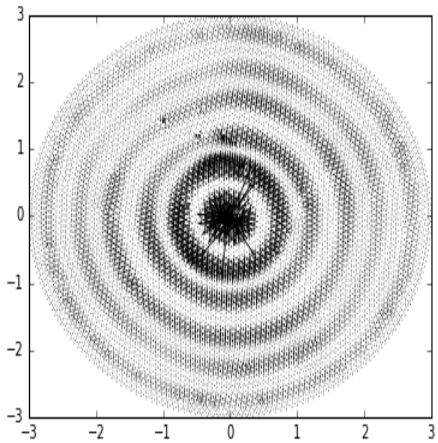

Figure 10: Velocity:t=3

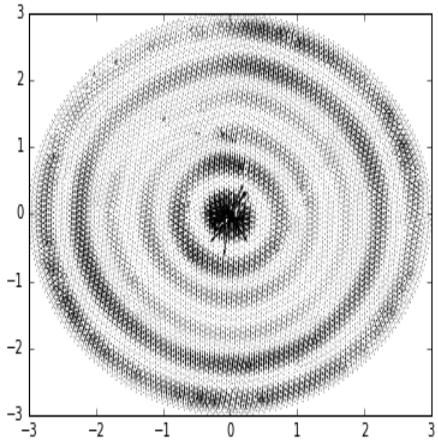

Figure 11: Velocity:t=4

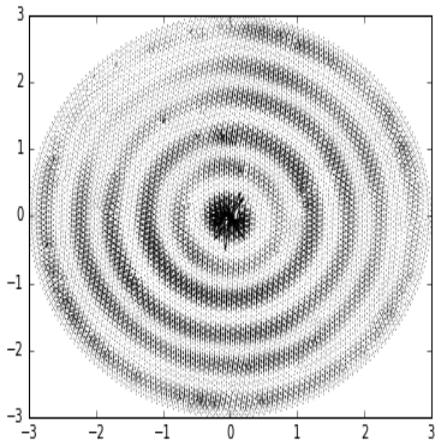

Figure 12: Velocity:t=5

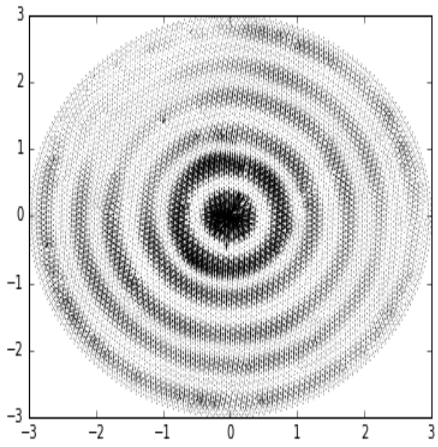

Figure 13: Velocity:t=6

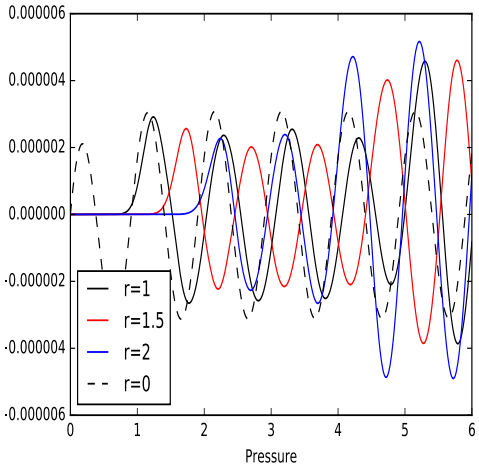

Figure 14: Comparison between pressure variation recorded at various radial locations (r=1, 1.5 and 2) and the source disturbance (r=0)

As seen here, the pressure variations are in-phase (barring the slight shift) at r=1 and 2 and out of phase at r=1.5 with respect to the source signal. This is to be expected as the wavelength of the signal $\lambda = a_0/f = 1$.

A better plot to check the frequency match between the source and the sampled signals is through the power density spectrum of each signal to identify the dominant frequency (shown in figure 15). As seen here, all three plots show the same dominant frequency of 1Hz. Some noise is also picked up by the samples, possibly due to error propagation through the temporal or spatial discretizaltion

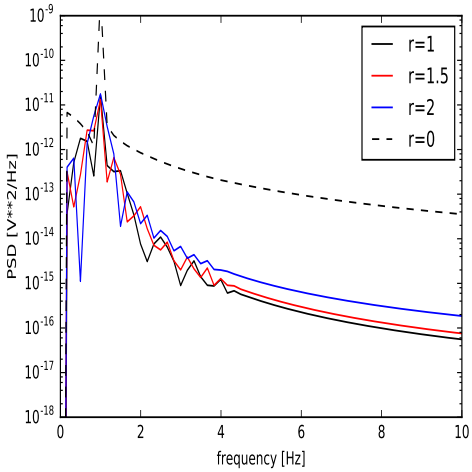

Figure 15: Power density spectrum of the source (r=0) and three samples (r=1, 1.5 and 2)

7. References

[1] Moshe Israeli and Steven A. Orszag. Approximation of radiation boundary conditions. *Journal of Computational Physics*, 41(1):115 – 135, 1981.

[2] A. Mani. On the reflectivity of sponge zones in compressible flow simulation. *Center for Turbulence Research, Annual Research Briefs*, 2010.